A Practical Guide to Setting Up Diffusion Measurements Utilizing Pulsed Field Gradients – Expanded

Earlier this year, we introduced a white paper, A Practical Guide to Setting Up Diffusion Measurements Utilizing Pulsed Field Gradients. We are re-introducing the paper with additional material to include solids diffusion methods. The paper is now presented is in three parts. Part one is the original material – with parts 2 and 3 being new material.

Daniel Arcos, John Staab, *Bibhuti Das, Paul D Ellis, and F. David Doty

Part I. Introduction to diffusion measurements and application with a liquids probe.

Part II. Diffusion measurements with MAS and a Magic Angle Gradient (MAG).

Part III. Self-diffusion measurement of water and lipids in model membrane system.

Doty Scientific Inc
700 Clemson Road
Columbia SC 29229

* Bibhuti Das is now at Nalco Champion (an Ecolab Company),
11177 S Stadium Drive, Sugar Land, TX 77478.
Email: bibhuti.das@ecolab.com

Part I.

Introduction. Approximately 50 years ago the Stejskal and Tanner (ST) article[1] appeared in the Journal of Chemical Physics. That paper transformed the way diffusion measurements were made and it continues to be best way to obtain self-diffusion (as opposed to flow) constants from NMR spectroscopic measurements *via* pulsed field gradients or PFG. The purpose of this note is to introduce to the user how to make diffusion measurements using a gradient-coil-equipped probe manufactured by Doty Scientific. However, the discussion is general enough such that it should apply to any probe equipped with a gradient coil regardless of who manufactured the probe.

Diffusion measurements by NMR methods are as old as the spin echo experiment first introduced by Hahn[2] in 1950. Recall, the basic Carr and Purcell[3] spin echo (as modified by Meiboom and Gill[4]) experiment is a $\pi/2$ pulse followed a waiting time τ. After this time τ, a π pulse (90° phase shifted relative to the $\pi/2$ pulse) is applied. After an additional time τ the spin echo appears. If the amplitude of the transverse magnetization immediately after the $\pi/2$ pulse is denoted as I_0, then in the absence of diffusion and relaxation, the amplitude of the spin echo will be I_0. In the presence of diffusion (or significant transverse relaxation) the amplitude of the spin echo will be less than I_0. With a proper analysis of the signals resulting from the pulse sequence, molecular diffusion can be addressed and the resulting diffusion constants can be obtained.

The reader is encouraged to read the ST paper and a few of the selected references contained within the paper. Those papers are referenced here[5-6]. Additionally, due to the impact of the ST paper, several reviews exist which discuss the experiment in some detail. Rather than list them all, we have selected the Sinnaeve review[7], which we found instructive. The interested reader should refer to some of the references cited within this review[8-11].

The basic pulse sequence introduced by ST can be described with the following timing diagram:

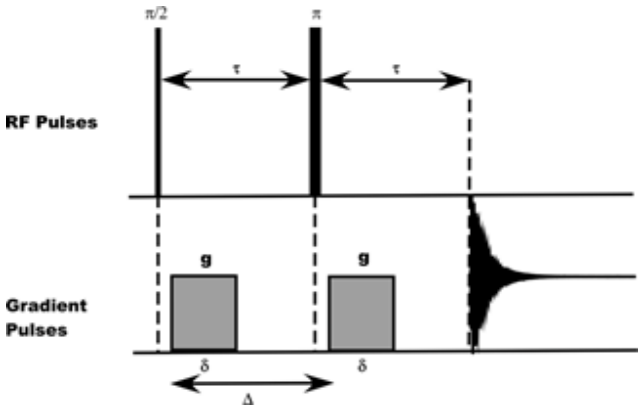

Figure 1. Simplified ST pulse sequence

In the absence of the gradient pulses, the timing diagram is simply that of a standard spin echo experiment, wherein after a time τ following a $\pi/2$ x-pulse the application of a π y-

pulse leads to the formation of an echo at a time 2τ. In the ST experiment gradient pulses on either side of the π pulse are added. In the now standard ST experiment the first gradient pulse of duration δ with amplitude g occurs at a time t_1 after the $\pi/2$ pulse. In the timing diagram above the time t_1 (not shown above) is a short recovery time after the rf-pulse and before the gradient pulse is turned on. In our experiments (using our JEOL ECA Spectrometer), t_1 is set to 100 μs. (As shown in the ST paper, the choice for t_1 has essentially no effect as long as it is short compared to τ and greater than the rf recovery period.) This sequence is often referred to as a pulsed gradient spin echo (PGSE) sequence.

Using the notation within the Sinnave review, the equation describing the intensity I loss in the ST experiment due to diffusion compared to the absence of diffusion and zero gradient is given by:

$$\ln\left[\frac{I_{2\tau}}{I_0}\right] = -D\gamma^2\delta^2 g^2\left(\Delta - \frac{\delta}{3}\right) \qquad [1]$$

The relative intensity loss only depends upon the diffusion coefficient, *D*, and several parameters under experimental control – the strength of the gradient g and the timing variables Δ and δ. The above expression is accurate for unrestricted diffusion and rectangular gradient pulses for $\delta <\sim \Delta/3$ and $g >> g_b$, where g_b is the mean background gradient (from imperfect shimming and gradient eddy currents) during the evolution period. The gyromagnetic ratio is precisely known. The only parameter that may not be accurately known is the strength of the gradients, g.

In the derivation of Eq. [1], we utilized a gradient pulse of constant amplitude, a half square wave. If the experiment was carried out with another form for gradient pulse, Eq. [1] would have to be changed. A common shape for a gradient pulse is a half sine wave.[7, 8] The solution for this case, in which the peak gradient g is the same, is well known. If we identify the terms other than the diffusion constant, as q, then we have:

square wave: $q = \gamma^2 g^2 \delta^2 (\Delta - \frac{\delta}{3})$

half sine wave: $q = \left(\frac{4}{\pi}\right)\gamma^2 g^2 \delta^2 \left(\Delta - \frac{\delta}{4}\right)$.

Here the symbols have the same meaning as described in Eq. [1].

Determination of the Strength of the Gradient, g.

For our purposes here, we have utilized a Doty PFG Probe for liquid samples (5 mm ^{1}H observe, with a lock channel). The gradient assembly is composed of the various coils that make up the gradient system but also includes an rf-shield (to permit predictable rf tuning) done in a way that prevents eddy currents from interfering with the experiment. The assembly utilized in our experiments is denoted as a 16-38 Z coil. The 16-38 refers to the approximate ID (mm) and OD (mm), respectively of the gradient coil assembly (the actual ID includes the rf-shield as well). The "Z" refers to the direction of the gradient, in this case along the axis of the main magnetic field. The RMS gradient non-uniformity over a 6X12 mm cylinder is approximately 3%. We note that many others have often

(improperly) denoted the maximum deviation of the B field from that produced by a perfectly constant gradient as the “gradient non-linearity” rather than using the technically accurate nomenclature “maximum relative field error”. (The ideal gradient is not linear, but rather is a constant. It is the field that is linear.) For comparison, a gradient rms non-uniformity of 3% would typically lead to maximum relative field error (aka “gradient non-linearity”) of ~1.5%.

Additional coil parameters are needed to select a suitable amplifier and to determine rise time and gradient strength. These include the resistance and inductance of the coil, 1.9 Ω and 158 μH, respectively, and what is most commonly called “gradient efficiency”. (We have previously preferred other terms, including gradient gain or gradient coefficient, as this number isn’t dimensionless, as efficiencies normally are). For the 16-38Z, the expected mean gradient “efficiency” (we are coming around!) is 472 mT/m/A for the above mentioned 12-mm sample length. (The gradient decreases slowly away from center, so the average value will be less for a longer sample but a little greater for a shorter sample – expected to be 477 mT/m/A for any sample length under 9 mm. In addition, there may be ~1.5% manufacturing variation in these numbers. The resistance is rather temperature dependent and may be 15% larger if the maximum allowable gradients are generated.)

The resistance of the coil is an important parameter and deserves more attention. The resistance can be measured by two approaches: a normal two-point or four-point measurement. The two-point (or two wire) method is simply using an Ohmmeter and measuring the coil resistance relative to ground. The four-point (or four wire) approach is slightly different. The four-point method is typically utilized when the lead resistance can significantly contribute to measured resistance of the object of interest in this case the coil resistance. The details of the two measurements can be found by simply “googling” four-point resistance measurement. When these measurements are performed, our two-point measurement yielded 1.9 Ω whereas a four-point measurement yielded 1.7 Ω. It is this latter value we will utilize in our subsequent analysis.

Utilizing these values, the experiment can be set up. The first thing to do is to make sure that when the output is supposed to be zero it really is very close to zero – down by more than a factor of a million compared to the gradient pulse! A diode blanking circuit may need to be connected in series with the Z-gradient line between the probe and amplifier to achieve sufficiently fast pulse settling.

Since the gradient is proportional to the current, gradient amplifiers generally operate in “constant-current mode” or “transconductance mode”, meaning their output current is proportional to their input voltage – so the temperature-dependence of the coil resistance doesn’t matter. (This mode also helps accelerate the large-signal portion of the pulse rise and fall.) The problem that arises is that in practice it is difficult to achieve very fast settling in a high-power amplifier operating in constant-current mode. It is not uncommon for gradient amplifiers to take anywhere from 0.1 ms to 2 ms for their outputs to settle to under 0.1 mA following a 20-A pulse. The time required to settle to such a low current is usually not important in simple diffusion experiments, but it often will be in DOSY experiments. Some gradient amplifiers have an output blanking circuit, but in some cases enabling it introduces a strange combination of offset drift and linearity problems that are sufficient to prevent some DOSY experiments with short Δ (even using bipolar pulse methods) from working as expected. (Be aware!, and suspect that this is the

problem if decay time is appearing to increase much more quickly than linearly with pulse current or duration.)

A diode blanking circuit, as shown in Figure 2, will often give best results when fast recovery is critical. The small value of R1 shown in Figure 2 has seemed needed for sufficiently fast settling in some cases, but it also has the undesirable effect of increasing the minimum threshold above which the gradient is proportional to the drive signal. A more optimum value in many cases may be 25 Ω . Note that Schottky rectifiers are preferred, and several will need to be paralleled to handle the high current.

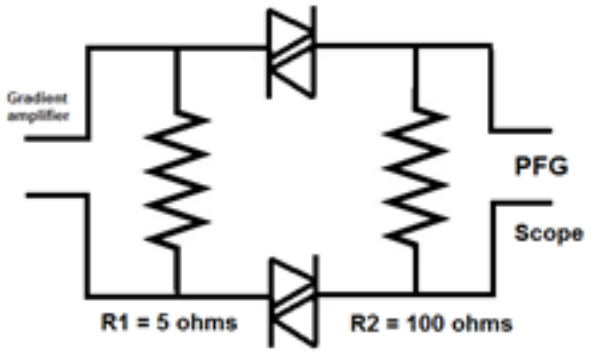

Figure 2. Diode Blanking Circuit

The remaining experimental details are spectrometer dependent. Somewhere, either within the pulse program or an explicit data file you must detail how the experiment is to be run. For example, you will need to set the values of the gradients used in the experiment. Typically, the experiment is operated such that normal relaxation (T_1 and T_2) processes are not changing during the experiment. Hence, by just varying the amplitude of the gradient pulse during the experiment some complications can be avoided.

The usual units for a field gradient are in mT/m. Depending upon the spectrometer software you can directly input the real values of the gradient or a voltage, which (ignoring for the moment some non-linearity at low values from the blanking circuit) is proportional to the field gradient. This value can be calculated by examining the pulse voltage going into the coil, which can be measured via an oscilloscope. Knowing the resistance of the Z-gradient coil (plus leads) and the voltage, the current can be calculated. The expected gradient strength (for 16-38 Z) is 477 mT/m•A near the center of the coil. So, the expected gradient strength in mT/m can be placed in the data file.

An experiment can now be performed which will enable an experimental value of the field gradient strength for the coil. For purposes of our calibration experiments we utilized a sample 4.1 mm length of water that at one time could be considered as “distilled” (not degassed) centered with *Ultem* susceptibility plugs. The experiment was set up using a JEOL calibration sequence for the calibration of the field gradient. The calibration experiment is a variation of the sequence summarized in Figure 1. To gain better understandings of the experiment consider subdividing the sample into and ensemble of thin horizontal planes. The thickness of a given plane is such that during the gradient stage of the experiment the Z-gradient appears to be constant within the plane. Application of a Z-gradient encodes the position of the spins within a given plane:

$$\upsilon(z) = \frac{1}{2\pi}\gamma[B_0 + g_z z]. \qquad [2]$$

First, let's consider the consequences of the on-resonance pulse sequence in the absence of diffusion and field gradients. Application of a 90° pulse produces transverse magnetization. In the absence of relaxation or diffusion the magnetization will simply stay within its transverse plane. Depending upon the offset frequency the transverse magnetization will simply precess within this plane about the Z-axis. This picture is the same for each member of our ensemble of planes. The application of a 180° pulse after a time τ reverses the direction of the precession for each member of the ensemble such that after an additional wait time of τ the spins have refocused. As previously discussed, this is simply a spin echo experiment.

Again, in the absence of diffusion and relaxation consider the application of a linear gradient along the Z-axis after the initial 90° pulse. The precession frequency of the transverse magnetization within a given plane depends upon the value of the field the spins experience within that plane. The applied gradient makes the field different in each plane. Hence, the presence of the gradient has the effect of encoding the z-position of each spin within a given plane. After a time τ a 180° pulse is applied. As before this pulse has the effect of reversing the sign of the precession frequency for spins in each plane. After a time τ all of the spins have refocused. This is simply a spin echo experiment in the presence of a field gradient.

If we examine spins in two distal planes we see that in the presence of the gradient the spins are wound about the Z-axis with a transverse frequency, which is proportional to the gradient's field within their respective planes. It is the symmetry of the basic spin echo sequence that allows the spins to come back to their initial position (again in the absence of diffusion and relaxation). Consider the consequences of intentionally breaking that symmetry. We can accomplish this by simply making the applied gradient during the second half of the experiment different than that in the first half. This is what happens in a gradient calibration experiment.

Breaking the symmetry means at the end of the second τ value the spins in the various planes are still experiencing the applied gradient within that plane. Acquiring the "echo" with normal processing yields the spectrum whose line width reflects the distribution of spins.

A better way to visualize the breadth of the gradient is to leave the gradient on during the acquisition. Under these conditions, the spins are simply precessing around the Z-gradient field. As such, the spins are spread out in frequency space that reflects the strength of the applied gradient. Below is the result of such an experiment, where the applied current was 1.86 A. After normal processing, a spectrum similar to the one illustrated below is obtained. The apparent "foot" in the spectrum is an artifact of not having the sample perfectly confined by the susceptibility plugs to the central region (some sample is above and below them, and some on their sides), but it does not affect the result. (If the rf coil is sensitive in the region where the gradient vanishes, which is 12 mm from the center for the 16-38 coil, and if sample is present there, you can expect to see a large narrow artifact near the center of the spectrum.) It is also important that the sample be centered with respect to the receiver coil. With these assumptions in mind and Eq.2, the gradient calculation is fairly straightforward. Dividing the computed gradient (g or g_z) by the applied current yields the gradient coefficient (G or G_Z). Hence,

based on the length of the sample (dimension in the Z direction, or 4.1 mm), the current applied (1.86 A) in this experiment, the bandwidth of the signal measured at the midpoint of the steep sections of the curve (~151,655 Hz), and the gyromagnetic ratio of proton [$(\gamma_H/2\pi)$ = 4258.9 Hz/G], the gradient strength from the spectrum shown is 151,655/4258.9/.41 = 86.85 G/cm or 868.5 mT/m. Correspondingly, the gradient **coefficient is 46.69 G/cm/A or 466.9 mT/m/A. The factory estimated value for the** gradient coefficient was 477 mT/m/A. The difference is on the order of 2%. Given the preceding discussion, the level of agreement is what is expected.

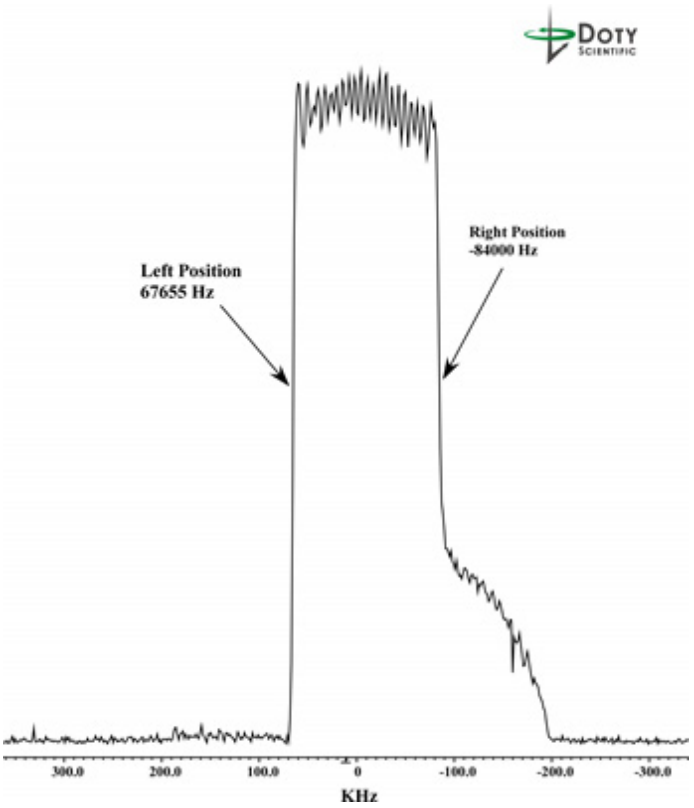

Figure 3

Keeping in mind we want to determine the diffusion constant of protons in our water sample, we have one more piece of housekeeping to address. In creating the data file used for the diffusion experiment we did not input each point in the units of mT/m. Rather, we simply input the data as voltage measured via the oscilloscope. The spectrometer labeled those voltages as mT/m. Hence, we need to determine the constant of proportionality between voltage and the real values of field gradient applied. This can be accomplished by at least two ways. The first and perhaps the easiest method is to compute the constant from the voltage used in the experiment that gave rise to the spectrum depicted in Figure 3. The voltage input was 2.82 V. From the JEOL software 2.82 V corresponds to 18 “mT/m” (JEOL Units). This value provides the means to calibrate the real value as opposed to the artificial value. In this case the scale factor is 868.5/18 or 48.25.

Determination of the Diffusion Coefficient, D, for water

The diffusion coefficient D can be evaluated from formula (1) by changing either the strength of the magnetic field gradient g, the duration of the field gradient pulse δ, or the time between the two magnetic-field gradient pulses Δ. As mentioned previously, in the measurement in which a time parameter such as the duration of the field gradient pulse δ or time between pulses Δ changes, you have to consider other time influences, such as relaxation. Therefore, the measurement by changing magnetic-field strength, g, is presently in general use.

To determine the diffusion constant of water, we have utilized our previous water sample used to calibrate the gradient strength. The resulting semi-log plot of $\gamma^2\delta^2 g^2(\Delta - \delta/3)x10^6$ *vs* $\ln(I/I_0)$ is given in Figure 5 for the water sample at ~21 °C. Slope of data is calculated to be 4.58 x 10^{-6} m^2/s. Using the calibration factor determined previously, 48.25, the computed value of the diffusion coefficient is 1.97 x 10^{-9} m^2/s. This value is similar to the one found by Holz and coworkers [10]. Holz and coworkers obtained D value of 2.025x10^{-9} m^2/s for a highly purified water sample at 20 °C. Our water sample had not undergone any polishing as described by Holz and coworkers. Hence, we consider the agreement with our measured value to that of Holz to be excellent.

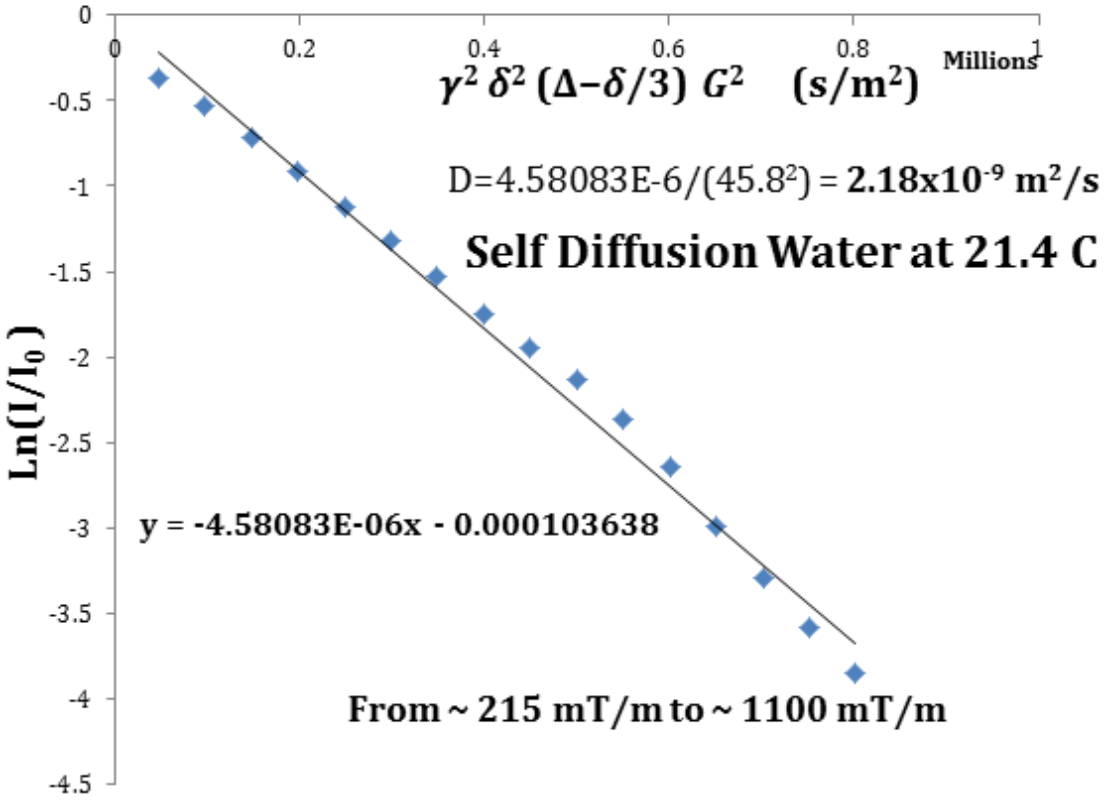

Figure 4

By changing the sequence timing and/or the gradient strength the experiment can be utilized to measure diffusion constants for much larger molecules. Many of the suggested experimental details can be found in manuals for your spectrometer.

Part II. Measuring Diffusion with MAS NMR.

Self-diffusion measurements of large macromolecules in solution are more difficult due to slow molecular tumbling, which in turn introduces complex relaxation mechanisms that broaden resonance peaks. Hence, poor resolution and sensitivity can introduce bottlenecks in diffusion NMR applications. An alternative method to improve resolution and sensitivity is to spin the sample fast enough at the magic angle (54.7°), which (at least mostly) removes the anisotropic interactions introduced by slow motion. As a result, high-resolution MAS (HR-MAS) techniques are often employed for studying molecular diffusion in biological tissues and in heterogeneous viscous liquids.

The advent of magic angle gradient (MAG) HR-MAS probes has increased our ability to utilize MAS NMR techniques in a number of applications in solution, viscous liquids, and solids as well. Moreover, many applications of PFGs may be improved considerably by using magic angle spinning. These include solvent suppression, reducing T_1 noise artifacts, sensitivity enhanced experiments with efficient coherence pathways selection, diffusion coefficient measurements, and diffusion-weighted spectral editing. In this section, we focus on the performance of self-diffusion measurements under MAS using commercially available HR-MAS-MAG probes from Doty Scientific. These probes have several advantages: (1) Low-E cross-coil resonators that are optimized for inverse proton detection and reduce RF heating during ^{1}H decoupling by 30-fold in biological samples; (2) High resolution ^{1}H NMR (under 2 Hz full width at half maximum from dilute water or organic solvents); (3) high power MAG coil, permitting up to 500 G/cm along the spinning axis with negligible off-axis components; (4) Fast gradient switching and minimal gradient recovery time, enabling implementation of rotor synchronized pulse techniques; (5) High power RF performance, enabling solids applications under MAS up to 24 kHz.

Utility of magic angle gradients.

It has been shown for quite some time now that multiple quantum echoes (MQEs) are produced by highly polarized solvents in the presence of small magnetic field gradients. These spin echoes produced by non-vanishing dipole-dipole couplings are NMR detectable and have been previously described using quantum mechanics. The magnitude of this gradient-induced echo signal S_n with respect to the single quantum signal after a 90° rf pulse is given approximately by[13,14]

$$\frac{S_n}{S_1} = 0.25 * t2 * \frac{[3cos^2\theta - 1]/2}{\gamma\mu_0 M_0} \quad , \qquad [3]$$

where $\gamma\mu_0 M_0$ is the dipolar demagnetization field, θ is the angle between the gradient vector and the magnetic field, and t_2 (here) is the acquisition time. Interestingly, the echo signal intensifies with increase in acquisition time according to Equation [3] and maximizes when the gradient field vector is parallel to the static magnetic field. In practice, strong solvent (water) signals produce MQEs, which may also interfere with clean coherence selection in one and multi-dimensional NMR experiments. This is particularly critical in biomolecular NMR, where quantification of local dynamics in proteins are regularly carried out using single and multiple quantum coherence pathways in tailored experiments. Fortunately, the echo signal depends on the angle between the total gradient vector and the magnetic field B_0, as shown in Equation [3], and completely vanishes at a magic angle (54.74°) as shown experimentally by Bowtell and others.[15, 14].

In solution NMR a gradient field along the magic angle is sometimes created using three orthogonal field gradients, Gx, Gy, and Gz. The effective gradient angle is given by

$$\cos(\theta) = \frac{G_{iz}}{G_{total}} = \frac{G_{iz}}{\sqrt{G_{ix}^2+G_{iy}^2+G_{iz}^2}} \quad [4]$$

where i (=1,2, 3…) is the quantum number. (Note that the total gradient strength increases with increasing quantum number.) Hence, with such gradient coils, equal amount of field gradients along the three axes will produce a magic angle gradient. Single gradient coils on a former aligned with the z-axis can also be designed to produce a gradient at the magic angle[14], but both the 3-coil and the single z-aligned-coil approach are seldom capable of more than 80 G/cm, which is quite limiting for solids and macromolecule applications. In contrast, the Doty MAG coil, on a former aligned with the spinning axis and just large enough to accommodate the needed MAS sample coils, is uniquely able generate the gradient strengths needed for solids applications.

Effective solvent suppression by magic angle field gradients.

Solvent suppression is an important step in biological NMR applications, especially for proton detected experiments. Because the concentration of solvent protons are typically 10^4-10^5 times higher relative to solute protons in a typical sample, the spectrometer receiver gain optimizes for the heavily weighted water signal. As a result, solute signals are reduced during the measurements. Additional difficulties come from the broad baseline of the water signal that hinders resolution and quantification of NMR signals in either one- or multi-dimensional experiments.

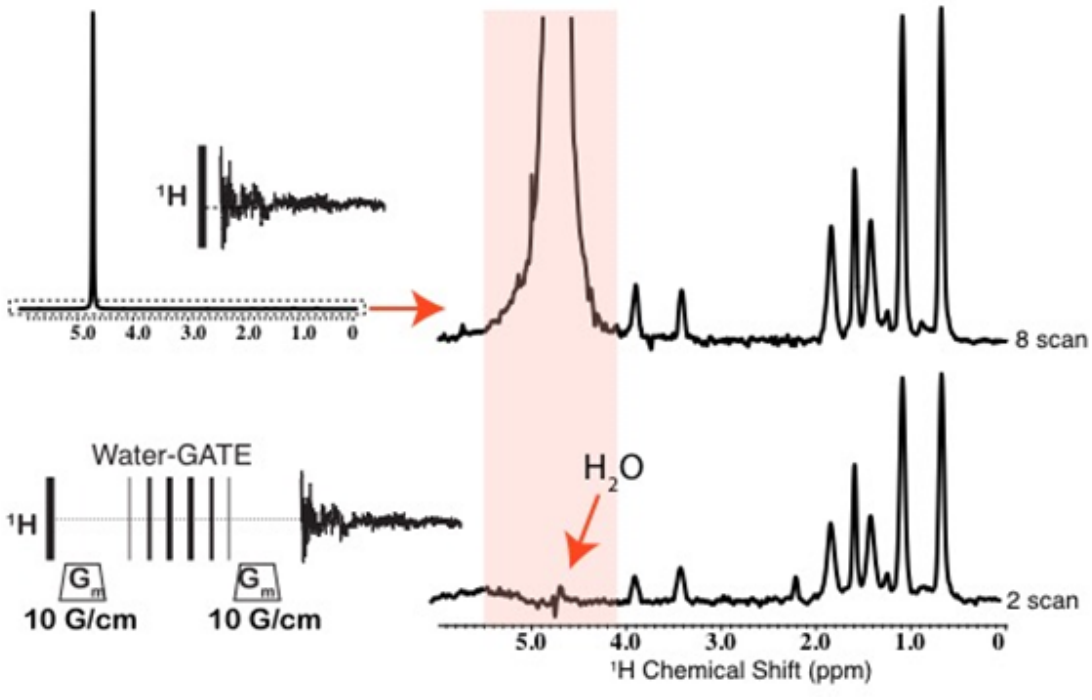

Figure 5: Water suppression using magic angle gradient pulses. 300 MHz ^{1}H spectra from ^{13}C labeled leucine dissolved in water were obtained under 4 kHz MAS.

The radiation damping (broadening) of the bulk water signal can have a number of deleterious effects in NMR spectroscopy: It (1) reduces magnetization transfer when studying Overhauser effects for protein-water and protein-drug interactions; (2) increases T_1 noise in multi-dimensional experiments; and (3) interferes with relaxation time measurement needed for quantification of local dynamics in proteins. The residual water signal is destroyed much more efficiently by using magic angle field gradients that with z-gradients only. It is important to note that water suppression is efficient even at as low as 10 G/cm total gradient strength (G_{total}) at magic angle. Experimental demonstration of water suppression using a WATERGATE pulse scheme[15-17] is shown in Figure 5.

A Low-E magic angle gradient MAS probe for inverse ^{1}H detection and self-diffusion measurement in water.

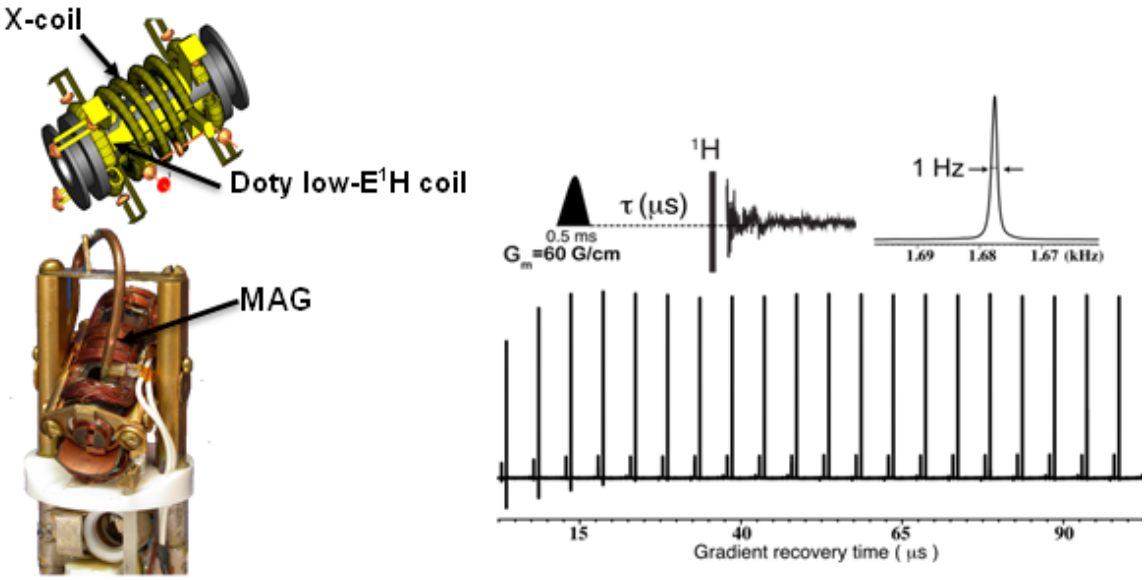

Figure 6: High-resolution MAS-MAG probe with Low-E RF resonator (left). Single pulse ^{1}H NMR of dilute water, pulse sequence for gradient recovery test, and experimental data are shown to the right. 60 G/cm SINE wave gradient pulse is applied for 0.5 ms.

Diffusion MAS NMR technique is a powerful tool for the measurement of self-diffusion coefficient in viscous samples or biological tissues, but one must be mindful of a number of details, including 1) MAS induced frictional heating, 2) RF and gradient field inhomogeneity; 3) possible axial rotor vibration during MAS; 4) possible RF heating during decoupling, and 5) possible sample convection driven by thermal gradients. Additional restriction applies to minimizing axial vibration in rotors because they cause phase incoherence under application of field gradients. In order to evaluate and address issues related to sensitivity, resolution, gradient linearity, and rf heating, doubly tuned (H/X, X for any nuclei below ^{31}P resonance frequency) or triply tuned (H/X/Y, X and Y are broad band frequency channels) MAS probes configured with low-E ^{1}H coils were examined. As shown in Figure 6, a low-E proton coil is wrapped around a coil form (i.e.,

the stator), thus maximizing filling factor for optimal proton detection. A multi-frequency tunable solenoid coil is over that. Additionally, a MAG coil is placed outside of the rf coils enabling pulsed field gradients along the rotor axis. For preliminary NMR tests on the probes, a narrow bore 4 mm MAS probe was tuned to 300 MHz proton and 75 MHz carbon frequencies. Experimental results are summarized in Figure 6. Experiments were performed on a dilute doped water sample (1-2% H_2O in D_2O, 0.2 mM $NiSO_4$) spinning 3-5 kHz MAS. The measured ^1H line-width at half maximum was ~1 Hz (0.003 ppm), with baseline widths of 10 Hz (~0.03 ppm) at 1% and 30 Hz at 0.1% of the water peak height.

Results from two gradient strength experiments are depicted in Figure 7, in which constant gradient current was applied during the acquisitions and the spectra were recorded. The experiment on the right, with a 6-mm length of water in the center, yielded a spectral width of 19 kHz. The gradient coefficient α, in mT/A/m, is given by the following:

$$\alpha = 1000 * \frac{\Delta f}{\gamma' I x}, \qquad [5]$$

where Δf is the signal width in kHz, γ' is the magnetogyric ratio in MHz/T, I is the coil current [A], and x is the sample length in mm. From this, we see a mean gradient coefficient of ~300 mT/A/m (30 G/A/cm) over the central 6-mm region. In the experiment on the left, two discs were inserted into the water-filled rotor approximately as shown. This experiment, in which experimental uncertainties were greater, gave values a little smaller, partly because the gradient strength is beginning to fall off at distances more than ~2 mm from the center. That is also evident from the spectrum on the right in Figure 7, where the slight increase in signal amplitude with distance from the center is indicative of decreasing gradient, assuming other factors are constant – B_1 and sample. (Some features in the spectrum on the left may be from bubbles.) The probe reliably delivers up to 500 G/cm gradient pulses at a duty cycle below 5% with sufficient nitrogen gas flow (i.e., when spinning over 15 kHz) for the cooling of the gradient coil.

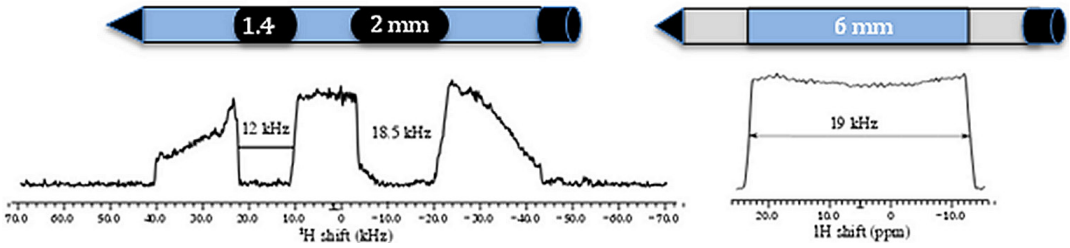

Figure 7: One-dimensional images of water obtained from gradient recalled echo experiments. Shown above the spectra are graphical illustrations of the samples. Left, 1.4 mm and 2 mm plastic discs in a rotor with water elsewhere; and right, a 6 mm long sealing cell. The CW currents during acquisition were 0.85 A (left), and 0.25 (right).

The single-pulse experiment shown in Figure 6, showed recovery time – to 90% of final amplitude – of less than 10 μs following a 0.5 ms mono-polar sine-wave gradient pulse of 60 G/cm peak for a case where the linewidth was ~50 Hz. Recovery time was significantly longer for square gradient pulses and for narrow lines. Recovery time also increased with amplitude and duration of the pulses, and it was not much shorter for bipolar pulses. Moreover, some baseline phase modulation in the signal persisted for 3-15 times longer than it took for the amplitude to recover to 90%, particularly on signals

where the linewidth was under 15 Hz. For example, in a case where the shimmed linewidth was 6 Hz, spinning at 4 kHz, with 1.2-ms bipolar sine-wave pulses of 420 G/cm, recovery to 90% of peak amplitude took 0.18 ms, and full decay of base-line phase modulation took ~2.5 ms. In all of these experiments, a diode box as described earlier (see Figure 2) was present.

Self-diffusion measurement of water under MAS

In this section, we discuss self-diffusion measurement of water under MAS. Sealing cells – either 50 μL or 20 μL – were used to confine the water to the middle of a 4 mm rotor, which was typically spun at 3-7 kHz. Experiments were conducted at 300 MHz ^{1}H frequency using a XC4 double tuned MAS probe equipped with a solenoid RF coil and a MAG coil. The strength of the MAG coil was calibrated using the above techniques, resulting in an experimentally measured gradient coefficient of 28 G/cm/A for a sample length of ~8 mm. A GRE or gradient spin echo experiment, similar to that used for Figure 7, was employed to confirm that the diode box did not significantly alter the expected constant relationship between actual gradient strength and spectrometer specified gradient over the range of interest. A graphical plot correlating the spectrometer input with calibrated gradient strength is shown below in Figure 8. Note that the scaling factor, which, among other parameters, depends on amplifier gain setting, is constant over this range and ~3.3, though it should begin decreasing at lower gradients than shown here, depending primarily on the choice of R1 in the diode blanking circuit of Figure 2.

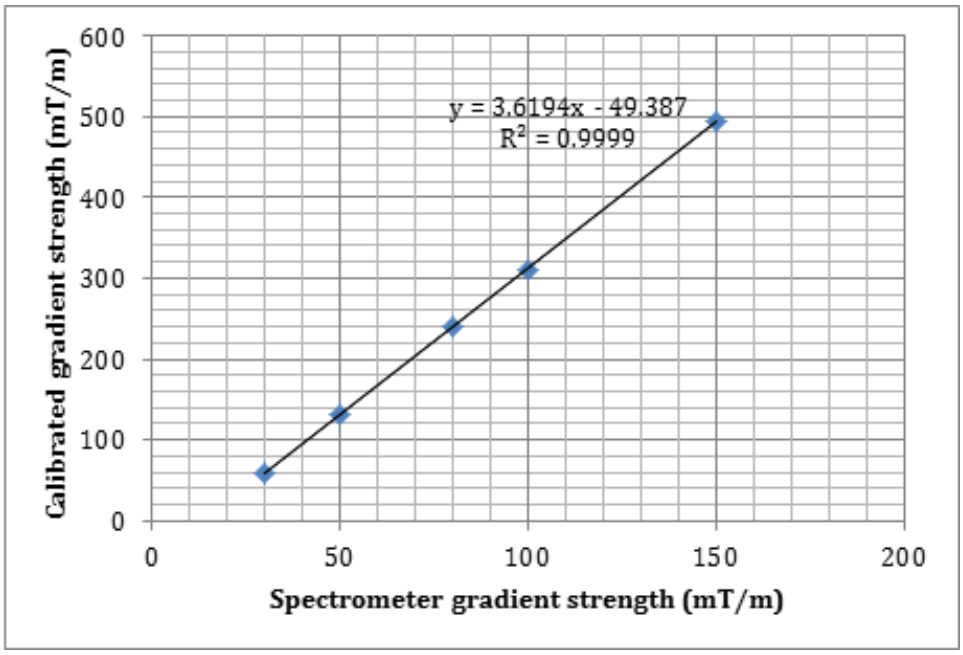

Figure 8: Correlation plot for spectrometer input gradient strength versus calibrated gradient strength for the MAG coil.

For the diffusion measurement, a spin echo pulse sequence was employed to measure the self-diffusion for a sample consisting of 2% water in 98% D_2O doped with 0.2mM $NiSO_4$. The resulting semi-log plot of $\gamma^2\delta^2 g^2(\Delta - \delta/3)$ *vs* $\ln(I/I_0)$ is shown in Figure 9 under ambient temperature. The JEOL Delta 4.3 software was used to fit the intensity curve to $\gamma^2\delta^2(\Delta - \delta/3)g^2$ (Ms/m^2, where M=1000) using the spectrometer value for g, which was then corrected by dividing by the square of the g scaling factor (3.3) as determined in Figure 8. Hence, the self-diffusion coefficient 2.18x10^{-9} m^2/s was measured for water at ambient temperature. Note that no rotor synchronization was needed and experiments were reproduced at spinning speeds up to 10 kHz.

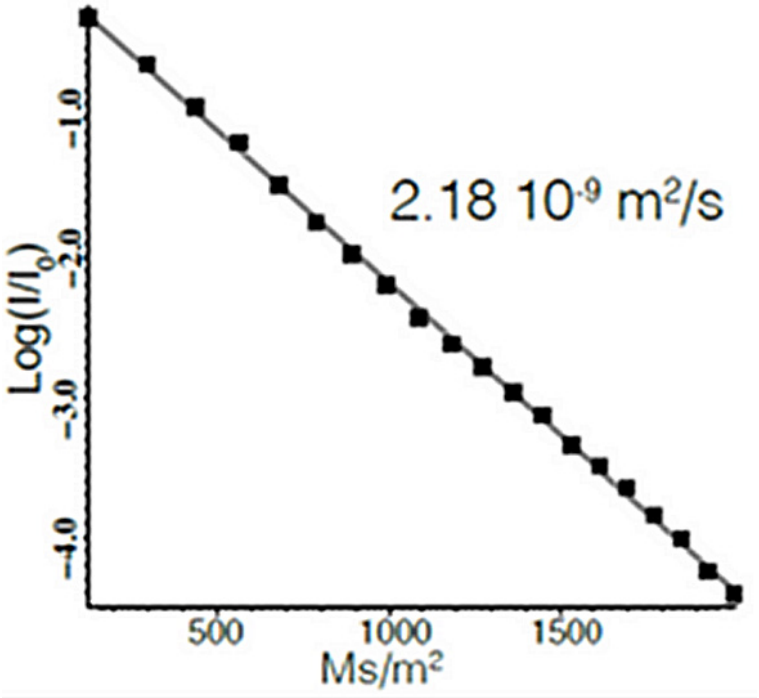

Figure 9: Logarithmic intensity correlation with $\gamma^2\delta^2 g^2(\Delta - \delta/3)$. γ:gyromagnetic ratio, δ: gradient pulse length (3 ms), g: gradient strength, Δ: diffusion time (20 ms). Experiment was carried out on a rotor containing 20 uL dilute doped water in a sealing cell, 4-6 kHz MAS, gradient strength was varied from 50 mT/m to 200 mT/m.

Part III. Self-diffusion measurement of water and lipids in unilamellar vesicles or proteoliposomes.

Diffusion MAS NMR is a reliable technique to gain understanding of the lipid, water, and protein dynamics in biological membranes. MAS enables proton detection with higher sensitivity. DSI high-resolution HRMAS probe optimized for inverse ^{1}H detection (low-E coil) was employed to measure self-diffusion coefficients in a proteoliposome sample. The proteoliposome sample was prepared by reconstituting a surface bound protein with Cytochrome C in unilamelar liposome vesicles prepared in excess water and DOPC/TOCL in a 4:1 ratio. Fast and slow diffusion rates of water at the interface of water, lipid and protein surface are shown in Figure 10.

Self-diffusion of bulk water in proteoliposomes is shown in Figure 10A. The diffusion coefficient obtained from a spin echo experiment measures 1.56 10^{-9} m^2/s. However, stimulated echo diffusion measurement in Figure 10B shows a nonlinear curve. The curve was deconvoluted using two separate diffusion coefficients of 1.56 10^{-9} m^2/s and 4.1 10^{-10} m^2/s. The initial portion of the signal decay is consistent with the bulk water diffusion rate and the second constant possibly belongs to the bound water (assuming there is a mixture). Hence, a water diffusion edited spin echo experiment was employed to measure very slowly diffusing water at the interface of protein, lipid, and water. That data, shown in Figure 10C, suggests two different diffusion constants, 6.0 10^{-11} m^2/s and 4.5 10^{-12} m^2/s. The first assumption would be water interacting with protein and on the lipid surface have different diffusion coefficients. There is also a possibility that curved surfaces modulate water diffusion. However, since we are using a short diffusion delay and high power gradient pulses, the effect is expected to be minimized but cannot be ruled out completely. *Water is believed to diffuse an order of magnitude faster on the surface of the lipid bilayer than in the lipids*. We also measured water diffusion in liposome samples and they agreed with the present result.

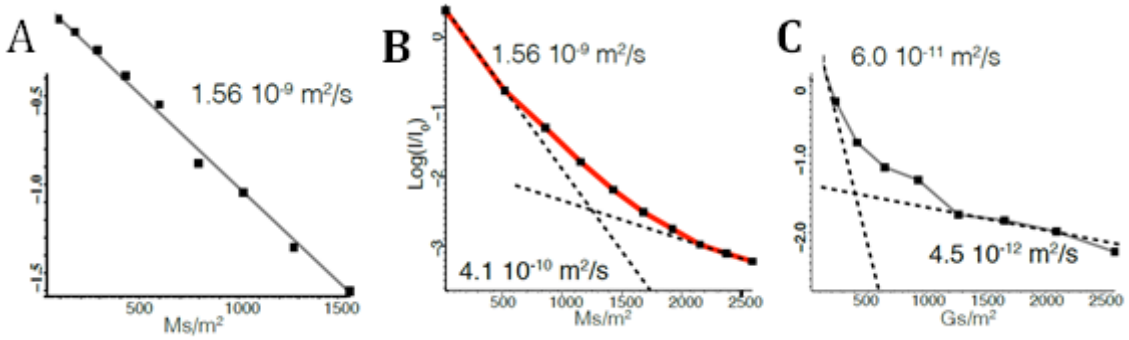

Figure 10: Self-Diffusion measurement of water at the interface of phospholipids and water. A. Spin echo measurement of bulk water with 40 ms echo delay. B. Stimulated echo (STE) measurement of bulk water signal. C. Water-diffusion-edited SE method to see the very slowly diffusing water at the interfaces.

The same methods can also be used to measure the diffusion coefficient of lipids in the liquid crystalline phase. However, to minimize error in diffusion coefficient measurement, stimulated echo (STE) experiments with bipolar PFGs were employed. STE provides better sensitivity compared to spin echo experiments. STE diffusion measurements from lipids also showed three separate diffusion coefficients measured from the deconvolution of peak intensity decay as a function of increasing gradient strength, as seen in Figure 11. Self-diffusion of lipids in hydrated bilayers is ~6.0 10^{-12} m^2/s (similar to our previous measurements and published data from other groups). However, lipids interacting with proteins are thought to have ~2-fold reduction in their mobility (1-1.1 x 10^{-13} m^2/s).

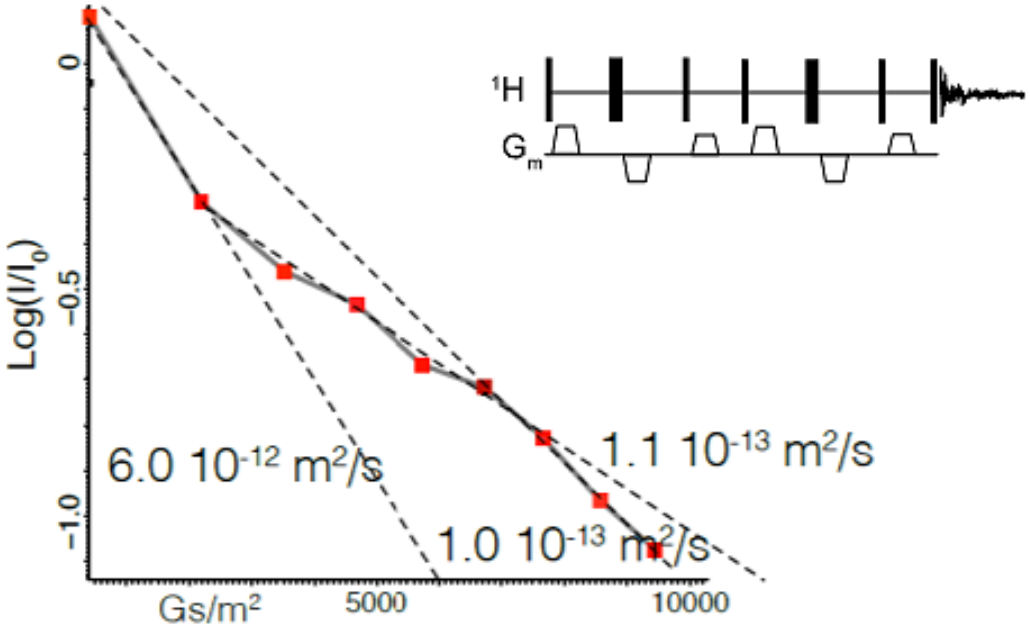

Figure 1: STE self-diffusion measurement of lipids in hydrated proteoliposomes at 20 °C and at 4 kHz MAS. Self-diffusion of lipids in hydrated bilayers is ~6.0 10^{-12} m^2/s. Lipids interacting with proteins have ~2-fold reduction in their mobility (1-1.1 10^{-13} m^2/s).

STE pulse scheme is shown on top. Thin and thick bars represent π/2 and π pulses, respectively.

Some Concluding Remarks.

Safety, Safety, Safety! The user of diffusion probes has to aware of the high DC currents (several amps) being applied to the probes required to generate the high field gradients. If used carelessly the probe can be damaged. Also, burns may be possible (though peak heating external to the coil is normally negligible). It is essential to read all of the user manuals and pay particular attention to the safety portions of the manual. For example, with water cooling, the model 16-38 Z gradient coil used in these discussions can handle

currents up to 62 amps with a 1.6% duty cycle, or 57.5 amps with 2.1% duty cycle. Alternatively, a continuous current of 8 amps could be used if water-cooling was employed. Currents half as large can be used with forced air cooling.

Finally, at Doty as part of our normal testing for PFG probes we determine the expected gradient strength, centering of the gradient, and the decay time after the gradient pulse. These tests are performed on either wide- or narrow bore probes within our wide bore magnets (either 7.05 or 11.7 T). Further, these tests unless specifically designed by the user, are performed "unlocked". We have never seen any evidence of significant interaction between the gradient coil and the shim coils, as the gradient coil is very accurately shielded. However, we have heard reports of unexplained artifacts/behaviors that may have arisen from interactions with a lock system that wasn't disabled. Very small B_0 eddy currents (sufficient to shift ^{1}H several Hz, with decay times of 10-100 ms) are unavoidable with high gradient pulses (they arise from minute winding errors). Hence, the end user should be concerned with the possible interaction between the gradient pulse and the timing of the pulse locks used on most high resolution spectrometers if the lock system is not disabled.

Acknowledgement

The authors wish to acknowledge several helpful discussions with Dr. Laura Holte during the preparation of this report. BBD would like to thank Dr. Patrick van der Wel and Dr. Mingyue Li at U. Pittsburgh for providing the proteoliposome sample.

References

1) Stejskal, EO, Tanner JE. Spin Diffusion Measurements: Spin Echoes in the Presence of a Time-Dependent Field Gradient. J Chemical Physics 1965; 42: 288. *doi.org/10.1063/1.1695690*

2) Hahn, EL. Spin Echoes. Physical Review 1950; 80: 580. *doi.org/10.1103/PhysRev.80.580*

3) Carr, H Y, Purcell, EM. Effects of Diffusion on Free Precession in Nuclear Magnetic Resonance Experiments. Phys. Rev. 1954; 94: 630. *doi.org/10.1103/PhysRev.94.630*

4) Meiboom S, Gill D. Modified Spin-Echo Method for Measuring Nuclear Relaxation Times. Rev. Sci. Instrum. 1958; 29: 688. *doi.org/10.1063/1.1716296*

5) Woessner DE. N.M.R. Spin-echo Self-diffusion Measurements on Fluids Undergoing Restricted Diffusion. J Physical Chemistry 1963; 67: 6: 1365–1367. *doi.org 10.1021/j100800a509*

6) Ardelean, I, Kimmich, R. Diffusion Measurements with the Pulsed Gradient Nonlinear Spin Echo Method. J Chemical Physics 2000; 112, 5275. *doi.org/10.1063/1.481123*

7) Sinnaeve, D. The Stejskal–Tanner Equation Generalized for Any Gradient Shape—An Overview of Most Pulse Sequences Measuring Free Diffusion. Concepts in Magnetic Resonance 2012; 40A: 39-65. *doi.org/10.1002/cmr.a.21223*

8) K. Nicolay, K. P. J. Braum, R. A.de Graaf, R. M. Dijkhuizen, and M. J. Kruiskamp, "Diffusion NMR Spectroscopy", NMR in Biomed. 14, 94-111 (2001). *doi.org/10.1002/nbm.686*

9) Holz, M, Weingartner, H. Calibration In Accurate Spin-Echo Self-Diffusion Measurements Using ^{1}H and Less-Common Nuclei. J Magnetic Resonance 1991; 92: 115-125. *doi.org/10.1016/0022-2364(91)90252-O*

10) Holz, M, Heil SR, Sacco A. Temperature-Dependent Self-Diffusion Coefficients of Water and Six Selected Molecular Liquids for Calibration in Accurate ^{1}H NMR PFG Measurements. Physical Chemistry Chemical Physics 2000; 20: 4740-4742. *doi.org/10.1039/B005319H*

11) Price, WS. Pulsed-Field Gradient Nuclear Magnetic Resonance as a Tool for Studying Translational Diffusion: Part I. Basic Theory. Concepts in Magnetic Resonance 1997; 9: 299-336. *doi.org/10.1002/(SICI)1099-0534(1997)9:5<299::AID-CMR2>3.0.CO;2-U*

12) Price, WS. Pulsed-Field Gradient Nuclear Magnetic Resonance as a Tool for Studying Translational Diffusion: Part II**.** Experimental Aspects. Concepts in Magnetic Resonance Part A 1998; 10: 4: 197-237 *doi.org/10.1002/(SICI)1099-0534(1998)10:4<197::AID-CMR1>3.0.CO;2-S*

13) *Waren, WS, Richter, W, Andreotti, AH, Farmer, BT II, Generation of Impossible Cross-peaks between bulk water and biomolecules in solution NMR Science, 262, 2005 (1993). doi.org/10.1126/science:8266096*

14) Zihl, PCM, Johnson, MO, Mori, S, and Hurd, RE, Magic-Angle-Gradient Double-Quantum-Filtered COSY, Journal of Magnetic Resonance, Series A, 1995; 113: 265-270**.** *doi.org/10.1006/jmra.1995.1092*

15) Bowtell R, Peters A. Magic-Angle Gradient-Coil Design. Journal of Magnetic Resonance, Series A, 1995; 115: 1: 55-59. *doi.org/10.1006/jmra.1995.1148*

16) Piotto M, Saudek V, Sklenar V. Gradient-Tailored Excitation for Single-Quantum NMR Spectroscopy of Aqueous Solutions. J. Biolmol. NMR, 1992; 2: 661-665. *doi.org/10.1007/BF02192855*

17) Sklenar V, Piotto M, Leppik R, Saudex V. Gradient-Tailored Water Suppression for ^{1}H-^{15}N HSQC Experiments Optimized to Retain Full Sensitivity. J. Magn. Reson, 1993; 102A: 241-245 *doi.org/10.1006/jmra.1993.1098*

18) Liu M, Mao X, Ye C, Huang H, Nicholson JK, Lindon JC. Improved WATERGATE Pulse Sequences for Solvent Suppression in NMR Spectroscopy. J. Magn. Reson, 1998; 132: 125-129. *doi.org/10.1006/jmre.1998.1405*